Construction of Type-II Bi₃O₄Cl/BiOBr Heterojunction Photocatalysts with Enhanced Activity for Levofloxacin Degradation

Mengjuan Xie^a, Jingjing Xu^b

College of Environmental Science and Engineering, Nanjing University of Information Science and Technology, Nanjing, China axiemengjuan@163.com, bxujj@nuist.edu.cn

Abstract: Bi₃O₄Cl/BiOBr composite heterojunction photocatalyst was prepared using in-situ generation method. A number of characterisation techniques were used to examine the prepared material's crystal structure, microstructure, elemental content, and optoelectronic characteristics. By breaking down the antibiotic ofloxacin in the presence of visible light, the produced photocatalyst's degradation activity was investigated. According to the experimental findings, a composite photocatalyst has a higher degrading activity than a photocatalyst made of a single component. The optimal composite sample BBC-2 has apparent rate constants that are 4.3 times and 3 times higher than those of pure BiOBr and Bi₃O₄Cl, respectively. The 4 cycles of experiments indicate that the composite sample has good stability. According to the electrochemical test results, it was found that the Bi₃O₄Cl/BiOBr composite photocatalyst has good photo generated carrier separation efficiency and excellent charge transfer efficiency, thus exhibiting good degradation activity towards ofloxacin. Superoxide radicals and holes are the primary active species in Bi₃O₄Cl/BiOBr composites in photocatalytic tests, according to the free radical capture experiment. In addition, charge transfer pathways and mechanisms for enhancing activity were proposed through free radical capture experiments and band theory.

Keywords: Photocatalyst; Heterojunction; Ofloxacin; Bi₃O₄Cl; BiOBr

1. Introduction

Antibiotics are used to treat and prevent a wide range of diseases that are brought on by bacterial infections. Before entering the environment, antibiotics undergo partial metabolism, excretion through urine and feces, and partial treatment by wastewater treatment plants^[1]. There are many sources of antibiotic pollution in water bodies, including the pharmaceutical industry, animal husbandry, aquaculture, etc^[2].

The difficulty of treating antibiotic wastewater is high, with high treatment costs and complex composition. It is a difficult to degrade organic wastewater that cannot be completely treated by traditional physical or chemical methods alone. Because of its many benefits, including high oxidation activity, economic viability, and environmental friendliness, photocatalytic technology is regarded as a viable approach^[3].

The current main goal is to develop a photocatalyst that can efficiently synthesize and separate photogenerated carriers in order to degrade target contaminants. The catalyst must also have a sufficient ability to absorb sunlight. Thus, one way to solve the problem is to change photocatalytic materials^[4]. Common methods for material modification include precious metal deposition, element doping, and constructing heterojunctions.

BiOBr readily crystallizes into anisotropic two-dimensional (2D) nanosheets due to the interplay of strong in-plane covalent bonding forces and weak interlayer van der Waals forces. For the logical structural design of Bi-O and Br⁻, this layered crystal structure is appropriate. Nevertheless, problems like poor reduction ability, high electron hole pair recombination rate, and low quantum efficiency continue to plague BiOBr photocatalytic materials^[5]. The photocatalytic performance of BiOBr can be enhanced using common modification techniques. Bi₃O₄Cl is a new 2D bismuth-based oxychloride that has garnered significant attention in recent years for its great chemical stability, narrow band gap, and distinctive open crystal structure in the degradation of organic contaminants^[6]. Combining BiOBr and

Bi₃O₄Cl to construct a heterojunction is beneficial for removing antibiotics from wastewater. To our knowledge, the preparation and performance research of Bi₃O₄Cl/BiOBr composite photocatalysts have not been reported yet.

2. Experimental

2.1 Synthesis of samples

According to previous literature reports, BiOBr was prepared^[7]. 2 mmol of Bi(NO₃)₃·5H₂O were added to 30 mL of EG and stirred for 30 minutes. Then, add 2 mmol of KBr and stir for 30 minutes. Subsequently, transfer the thoroughly stirred solution to a 100 mL reactor and added 30 mL of ethylene glycol. React at 160 °C for 12 hours. The recovered items were washed three times with deionized water and ethanol, then dried at 60 °C for six hours.

Bi₃O₄Cl/BiOBr composite photocatalyst was prepared by in-situ growth method^[8]. 2 mmol of Bi(NO₃)₃·5H₂O were added to 20 mL of EG, denoted as solution A; 0.66 mmol of NH₄Cl were added to 50 mL of distilled water, denoted as solution B. Mix solution A and solution B for 15 minutes each. Then add solution B dropwise into solution A, add different masses of BiOBr, and stir for 1 hour. Place the mixture in a 100 mL reactor and react at 160 °C for 12 hours. The recovered items were washed three times with deionized water and ethanol, then dried at 60 °C for six hours. The obtained product is placed in a muffle furnace and calcined at 500 °C for 5 hours at a heating rate of 5 °C/min. Prepare pure Bi₃O₄Cl according to the above experimental steps without adding BiOBr. In this experiment, the added BiOBr was controlled at a mass ratio of 10%, 35%, and 45%, denoted as BBC-1, BBC-2, and BBC-3.

2.2 Characterization

The crystal structure of photocatalysts was investigated with an X-ray diffractometer (XRD-6100). The microstructure of photocatalysts was investigated using TEM and HRTEM. The elemental composition and chemical state of the produced materials were determined using Thermo Scientific K-Alpha X-ray photoelectron spectroscopy (XPS). The light absorption properties of the materials developed by the research institution were determined using UV visible diffuse reflectance spectroscopy (DRS) using BaSO₄ as the background and a testing range of 200-800 nm. At the same time, the photoelectric performance of photocatalysts was investigated utilizing Shanghai Chenhua Instrument Company's CHI-660D electrochemical workstation, which included transient photocurrent response (PC) and Mott Schottky Schottky (M-S). To investigate the electron hole recombination of samples prepared by the research institute, the fluorescence emission peak intensity of the material at a specific excitation wavelength was measured by fluorescence spectroscopy (PL), and the photocatalytic performance can be observed from this test.

3. Result and discussion

3.1 Characteristic description

X-ray diffraction (XRD) was used to study the catalyst's crystal structure. Figure 1 displays the XRD patterns of Bi₃O₄Cl and BiOBr pure samples, as well as composite materials BBC-1, BBC-2, and BBC-3 with different mass ratios. The image shows that the BiOBr diffraction peaks primarily occur 10.9°, 25.21°, 31.72°, 32.27°, and 57.20°, which corresponds to the (001), (101), (102), (110) and (212) planes, respectively. These peaks are entirely compatible with the BiOBr standard card JCPDS No.85-0862^[9]. The absence of any additional impurity peaks suggests that the preparation of high-purity BiOBr was successful. According to the standard card JCPDS No.36-0760 of Bi3O4Cl, the primary diffraction peaks of the material occur at 23.98°, 29.13°, 29.68°, 31.40° and 31.65°, which corresponds to the(21-1), (41-1), (411), (002) and (020) planes, respectively^[10]. For composite materials, their characteristic peaks are similar to those of pure samples BiOBr and Bi₃O₄Cl. With the increase of BiOBr content, the characteristic peak corresponding to Bi₃O₄Cl in the composite material weakens, and no impurity peaks representing other substances were detected, indicating that high-purity Bi₃O₄Cl/BiOBr composite samples have also been successfully prepared.

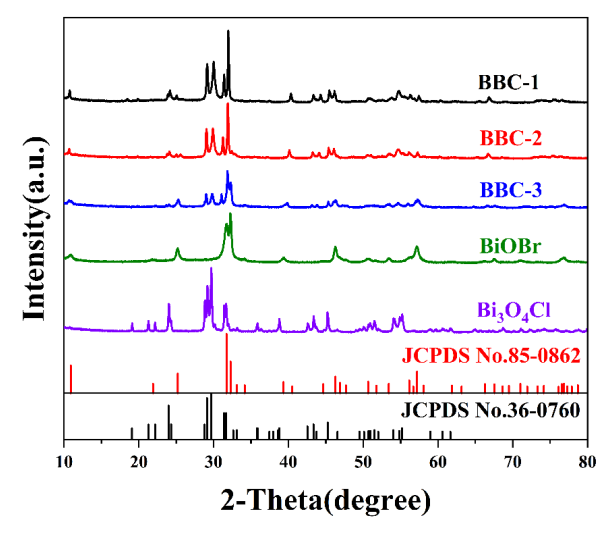


Figure 1: XRD patterns of Bi₃O₄Cl, BiOBr and BBC composite samples.

The morphology and structure of pure Bi₃O₄Cl, BiOBr, and composite sample BBC-2 were studied by TEM and HRTEM, as indicated in the figure. Figure 2(a) shows the synthesized Bi₃O₄Cl, which is a typical nanosheet shape with dimensions ranging from 300 to 500 nm. Figure 2(b) shows the synthesized BiOBr, which has an irregular nanosheet structure. Figure 2(c) shows the TEM image of the composite sample BBC-2, which clearly shows that the BiOBr sheet-like structure is tightly bound to the Bi₃O₄Cl nanosheets. The HRTEM picture of BBC-2 is seen in Figure 2(d), where two distinct sizes of lattice fringes are discernible. The (411) crystal plane of Bi₃O₄Cl has a wavelength of 0.301 nm, while the (102) crystal plane of BiOBr has a wavelength of 0.282 nm. The XRD and TEM/HRTEM results indicate that the BiOBr/Bi₃O₄Cl composite material has been successfully prepared.

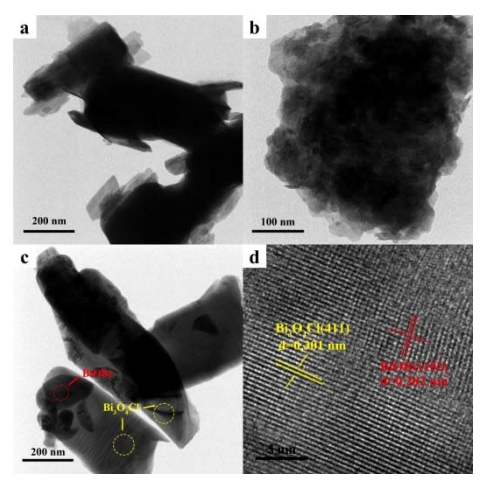


Figure 2: (a) TEM image of Bi₃O₄Cl, (b) TEM image of BiOBr, (c) TEM and (d) HRTEM image of BBC-2.

X-ray photoelectron spectroscopy (XPS) was used to examine the elemental makeup and chemical state in the photocatalytic materials that the institute produced. The primary peaks of Bi, O, Cl, and Br are clearly visible in the whole spectrum of BBC-2 in Figure 3(a), suggesting that the material includes appropriate elements and that the composite material has been successfully constructed. The Bi 4f spectra of BBC-2, Bi₃O₄Cl, and BiOBr are displayed in Figure 3(b). Compared with pure samples Bi₃O₄Cl and BiOBr, the two characteristic peaks of composite sample BBC-2 slightly shift towards lower binding energies^[11]. In BBC-2, Bi 4f_{7/2} and 4f_{5/2} have binding energies of 159.2 eV and 164.5 eV, respectively. Figure 3(c) displays the O 1s high-resolution spectrum. Lattice oxygen and oxygen adsorbed from the atmosphere are represented by the two fitted peaks at 530.1 and 531.6 eV, respectively^[12,13]. Br 3d spectra of BiOBr and BBC-2 are displayed in Figure 3(d). The Br element appears in the form of Br, and Br 3d_{5/2} and Br 3d_{3/2} equate to 68.3 eV and 69.1 eV, respectively^[14]. Cl 2p_{3/2} and Cl 2p_{1/2}'s binding energies in Bi₃O₄Cl are 198.3 eV and 199.9 eV, respectively, as Figure 3(e) illustrates^[10]. In addition, compared to Bi₃O₄Cl, the Cl 2p of BBC-2 moves towards a lower binding energy direction. Compared to BBC-2, Br 3d moves towards a higher binding energy direction. The

movement of binding energy is related to electron density^[15]. So there are interactions in Bi₃O₄Cl/BiOBr composite heterojunction materials that promote electron migration and conversion.

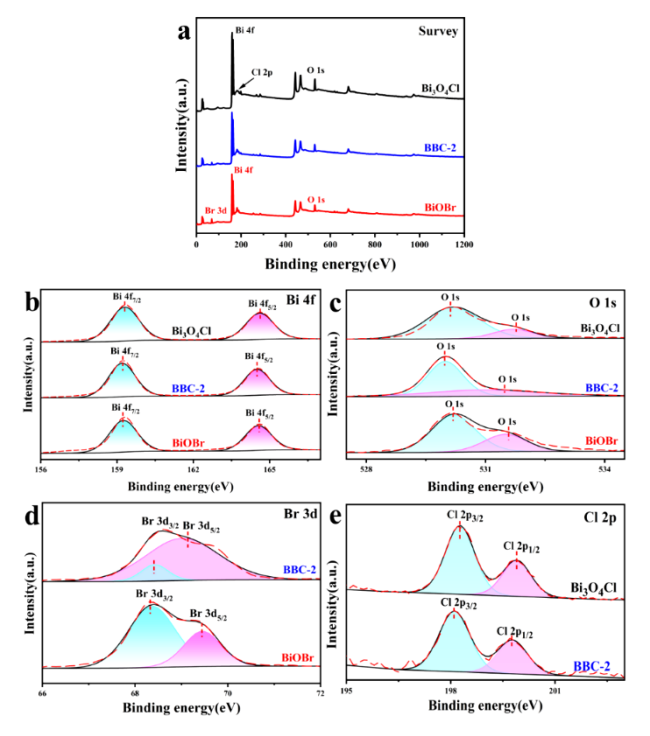


Figure 3: (a) XPS spectra of Bi₃O₄Cl, BiOBr and BBC-2; (b) Bi 4f spectra and (c) O 1s spectra of Bi₃O₄Cl, BiOBr and BBC-2; (e) Cl 2p spectra of Bi₃O₄Cl and BBC-2.

UV-vis-DRS was used on the samples to investigate the optical characteristics of the photocatalytic materials made by the institute. The absorption edges of BiOBr and Bi₃O₄Cl are 420 nm and 460 nm, respectively, as seen in Figure 4(a). The created composite material BBC-2 shows a notable red shift when compared to BiOBr, suggesting that the composite of BiOBr and Bi₃O₄Cl helps to enhance the material's responsiveness to visible light. For photocatalytic materials, the bandgap value can be computed with the following formula^[16]:

$$\alpha h v = A \left(h v - E_g \right)^{n/2} \tag{1}$$

The kind of optical transition in the semiconductor determines the value of n, which might be 1 or 4 for direct and indirect semiconductors, respectively. Literature research indicates that Bi₃O₄Cl and BiOBr are both indirect semiconductors^[17,18]. Consequently, it can be inferred from Figure 4(b) that the band gaps of BiOBr and Bi₃O₄Cl are 2.49 and 2.56 eV, respectively, which is in line with the findings of previous studies^[19,20].

In order to determine the conduction band (CB) of BiOBr and Bi_3O_4Cl materials, Mott Schottky tests were conducted. The tangent slopes of the M-S curves for BiOBr and Bi_3O_4Cl are both positive, as seen in Figures 4(c) and (d), suggesting that both compounds are n-type semiconductors. BiOBr and Bi_3O_4Cl have flat band potentials (E_{fb}) of -0.63 eV and -0.47 eV, respectively. Use the formula to convert E_{fb} to a conventional hydrogen electrode^[21]:

$$E_{\text{NHE}} = E_{\text{Ag/AgCl}} + 0.197 \tag{2}$$

The Fermi level (E_f) of n-type semiconductors is near the conduction band, and the minimum value of E_{CB} is approximately 0.1 eV higher than E_f . Consequently, -0.53 eV and -0.37 eV, respectively, can be computed as the E_{CB} values for BiOBr and Bi₃O₄Cl. Determine their E_{VB} by use formula (3)^[22]:

$$E_{VB} = E_{CB} + E_{g} \tag{3}$$

The reported values of 1.96 eV and 2.19 eV for BiOBr and Bi₃O₄Cl are in close agreement with their $E_{VB}s^{[23,24]}$.

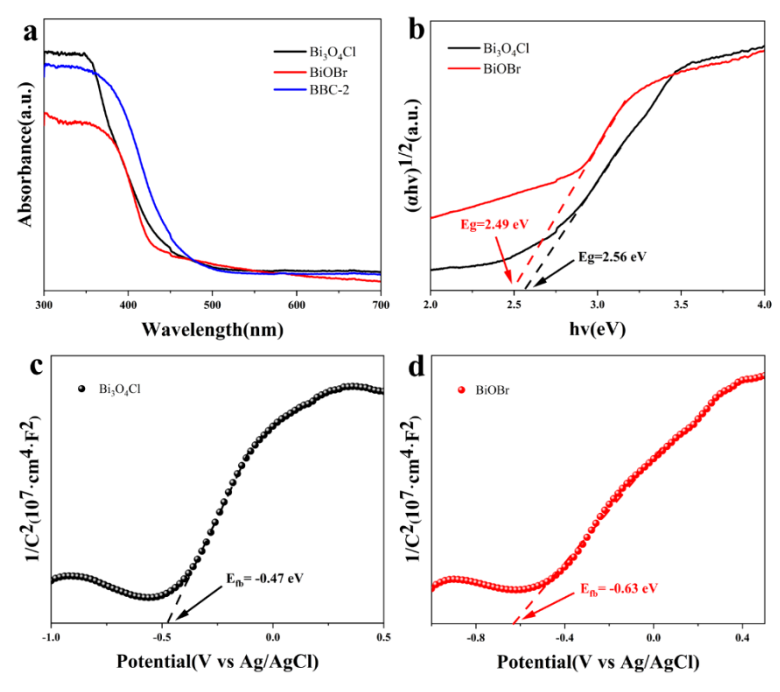


Figure 4: (a) DRS spectra of Bi₃O₄Cl, BiOBr and BBC-2; (b)images of αhv and v of pure Bi₃O₄Cl and BiOBr; Mott–Schottky (M–S) plots of (c) Bi₃O₄Cl and (d) BiOBr.

3.2 Photocatalytic performance

Under visible light, the research institute's composite samples of the Bi₃O₄Cl/BiOBr series were evaluated for their photocatalytic activity in degrading pollutants like ofloxacin. Dark treat the sample with pollutants for 40 minutes to achieve adsorption desorption equilibrium. Figure 5(a) illustrates how ofloxacin degrades in the presence of light. The pure Bi₃O₄Cl sample degrades at a rate of 44% in 20 minutes, while the pure BiOBr sample degrades at a rate of 34%. A single component photocatalyst has a limited capacity to absorb visible light, and its low deterioration rate is caused by the high rate of electron hole recombination. The degradation efficiency of composite sample BBC-1 towards ofloxacin within 20 minutes was 73%, while the degradation efficiency of BBC-2 and BBC-3 were 83% and 78.1%, respectively. The composite sample Bi₃O₄Cl/BiOBr exhibited superior photocatalytic activity compared to the pure sample. This suggests that the heterojunction construction successfully inhibited the recombination of photogenerated electron hole pairs and enhanced the rate of charge carrier migration. Among all composite samples, BBC-2 has the best photocatalytic activity. The photocatalytic activity will decline as the concentration of BiOBr increases, suggesting that too much BiOBr will prevent the composite material from absorbing visible light.

3.3 Photocatalytic mechanism

The effectiveness of electron hole migration and separation determines the photocatalytic efficiency of semiconductor materials. The more effective a substance is at separating and migrating electron holes, the higher its photocatalytic efficacy. The more effective a substance is at separating and migrating electron holes, the higher its photocatalytic efficacy. The efficiency of photogenerated carrier migration increases with photocurrent in transient photocurrent response testing. The photocurrent of Bi₃O₄Cl, BiOBr, and composite sample BBC-2 under visible light is shown in Figure 5(b). Bi₃O₄Cl and BiOBr have a weak response to light, while sample BBC-2 has a significantly stronger photocurrent intensity than the pure sample, indicating its good electron hole separation and migration ability, which is consistent with the results of photocatalytic activity degradation experiments.

Fluorescence spectroscopy is a characterization method that can reveal the recombination rate of photo generated electrons. The fluorescence spectra of Bi3O4Cl, BiOBr, and composite sample BBC-2 at 760-800 nm are shown in Figure 5(c). The order of fluorescence intensity is: BBC-2<Bi3O4Cl<BiOBr., The low electron hole recombination rate of BBC-2 composite material is the reason for the improved photocatalytic activity.

Free radical capture tests were carried out to identify the active species that are mostly responsible

for the breakdown of ofloxacin pollutants in Bi₃O₄Cl/BiOBr composite materials. The trapping agent for holes is ammonium oxalate (AO); The scavenger for superoxide radicals is p-benzoquinone (PBQ); And hydroxyl radicals are captured using isopropanol (IPA)^[25,26]. Superoxide radicals are a key player in the degradation process, as shown by Figure 5(d), which shows that the addition of PBQ dramatically inhibits the breakdown activity of ofloxacin. The addition of AO also partially hindered the degradation activity of ofloxacin, suggesting that holes were involved in the degradation process as well. After adding IPA, the degradation activity remained largely unchanged, indicating that hydroxyl radicals had little effect during the degradation process. Through capture experiments, we know that holes and superoxide radicals work together in the degradation process, with superoxide radicals being the most important.

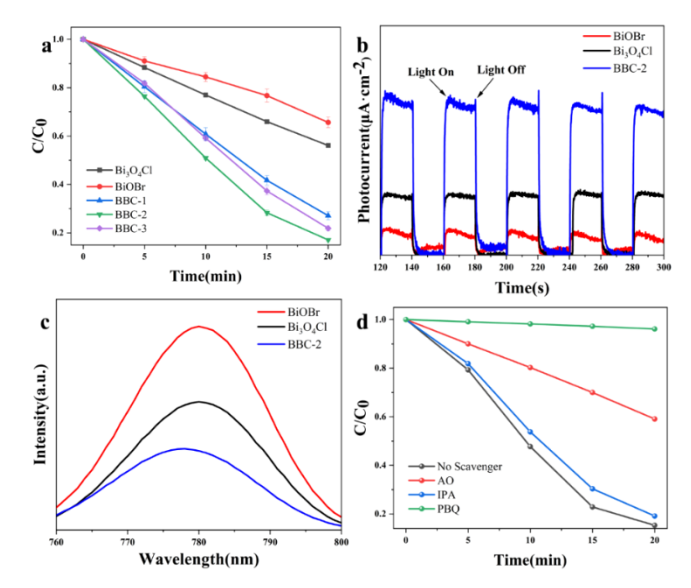


Figure 5: (a) Degradation curve of LVFX under visible light; (b) PC; (c) PL; (d) Effects of different scavengers on the LVFX photo-degradation by BBC-2.

Drawing from the aforementioned experimental findings, we suggest the mechanism of ofloxacin's Bi₃O₄Cl/BiOBr degradation, depicted in Figure 6. When the energy absorbed by the semiconductor is equal to or greater than the bandgap, the photo generated electrons on VB transfer to CB, leaving holes on VB. The BiOBr E_{CB} (-0.53 eV) in Bi₃O₄Cl/BiOBr materials is more negative than the Bi₃O₄Cl E_{CB} (-0.37 eV), while the Bi₃O₄Cl E_{VB} (2.19 eV) is more rectified than the BiOBr E_{VB} (1.96 eV). Positively charged holes in Bi3O₄Cl's VB can swiftly travel to BiOBr's VB, where they can degrade ofloxacin directly. Similarly, electrons in BiOBr's CB can swiftly move to Bi₃O₄Cl's CB. Because Bi₃O₄Cl has a lower generation potential (-0.33 eV vs. NHE) than $O_2/\cdot O_2^-$, some of the electrons can react with dissolved oxygen to produce superoxide radicals, break down ofloxacin, and produce tiny molecules that don't cause pollution, including H₂O and CO₂. The improvement of photocatalytic activity of composite materials is attributed to the construction of a type-II heterojunction between Bi₃O₄Cl and BiOBr, which greatly enhances the efficiency of photo generated carrier migration.

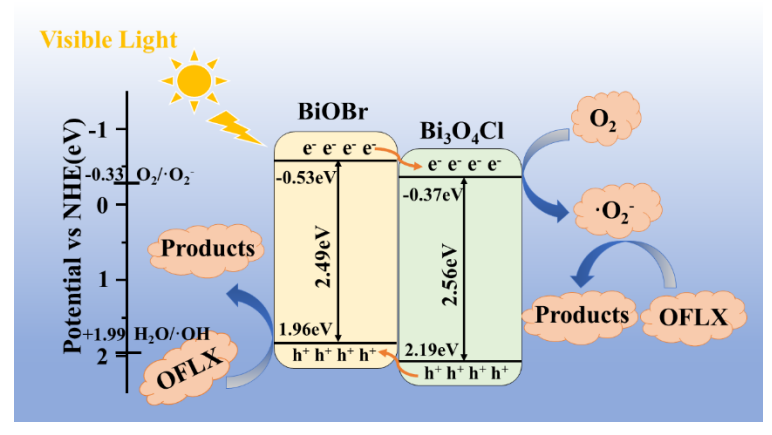


Figure 6: Charge transfer mechanism of Bi₃O₄Cl/BiOBr composite photocatalyst for degradation of ofloxacin under visible light

4. Conclusion

In summary, in-situ calcination proved to be an effective method for preparing the type-II Bi₃O₄Cl/BiOBr photocatalyst. The composite demonstrated outstanding photocatalytic degradation of LVFX in visible light, achieving an 83% degradation efficiency in just 20 minutes. The prepared material's crystal structure, microstructure, elemental composition, and optoelectronic properties were examined through the use of characterization techniques like TEM, XRD, XPS, DRS, and electrochemical testing. The charge transfer pathway and mechanism for enhancing activity were also suggested.

References

- [1] Li Z, Wen C, Li D, et al. Insights into nitrogen-doped BiOBr with oxygen vacancy and carbon quantum dots photocatalysts for the degradation of sulfonamide antibiotics: Actions to promote exciton dissociation and carrier migration[J]. Chemical Engineering Journal, 2024, 492: 152449.
- [2] Yang H, Zhang Z, Li J, et al. Visible-light induced ofloxacin photodegradation catalyzed by the S-scheme Bi₂MoO₆/NH₂-MIL-68(In) heterojunction: Interfacial engineering, DFT calculations, and toxicity assessment[J]. Chemical Engineering Journal, 2024, 487: 150554.
- [3] Zhou K, Liu W, Wang P, et al. Interfacial C-O covalent bonds improving the piezo-assisted photocatalytic performance of $Bi_4Ti_3O_{12}$ @Carbon Schottky heterojunction[J]. Chemical Engineering Journal, 2024, 480: 148012.
- [4] Zhang Q, Gong W, Che H, et al. S doping induces to promoted spatial separation of charge carriers on carbon nitride for efficiently photocatalytic degradation of atrazine[J]. Chinese Journal of Structural Chemistry, 2023, 42(12): 100205.
- [5] Qin F, Luo Y, Yu Q, et al. Enhanced charge transfer and photocatalytic activity of BiOBr/Bi₂WO₆ p-n heterojunctions[J]. Journal of Molecular Structure, 2024, 1304: 137719.
- [6] Ning S, Ding L, Lin Z, et al. One-pot fabrication of $Bi_3O_4Cl/BiOCl$ plate-on-plate heterojunction with enhanced visible-light photocatalytic activity[J]. Applied Catalysis B: Environmental, 2016, 185: 203-212.
- [7] Huang Q, Zhao Z, Zhao X, et al. Effective photocatalytic sterilization based on composites of $Ag/InVO_4/BiOBr$: Factors, mechanism and application[J]. Separation and Purification Technology, 2023, 327: 125011.
- [8] Huang L, Yang L, Li Y, et al. p-n BiOI/Bi₃O₄Cl hybrid junction with enhanced photocatalytic performance in removing methyl orange, bisphenol A, tetracycline and Escherichia coli[J]. Applied Surface Science, 2020, 527: 146748.
- [9] Yi M, Ren Y, Zhang X, et al. Ionic liquid-assisted synthesis of N, F, and B co-doped $BiOBr/Bi_2Se_3$ on Mo_2CT_x for enhanced performance in hydrogen evolution reaction and supercapacitors[J]. Journal of Colloid and Interface Science, 2024, 658: 334-342.
- [10] Li Y, Liu S, Huang L, et al. A novel Z-type heterojunction $Bi_3O_4Cl/Bi_4O_5I_2$ photocatalytic composite with broad-spectrum antibacterial activity and degradation properties[J]. Journal of Colloid and Interface Science, 2023, 652: 798-812.
- [11] Zhu Y, Shen K, Wang Y, et al. Controlled preparation of bamboo charcoal/BiOCl with efficient visible-light-driven photocatalytic activity for organic pollutant degradation using the residues of bamboo processing[J]. Industrial Crops and Products, 2024, 215: 118620.
- [12] Yu G, Sun Q, Yang Y, et al. S-scheme heterojunction construction of Fe/BiOCl/BiVO₄ for enhanced photocatalytic degradation of ciprofloxacin[J]. Progress in Natural Science: Materials International, 2024, 34(2): 290-303.
- [13] Nie Q, Jia L, Luan J, et al. Graphene quantum dots/BiOCl visible-light active photocatalyst for degradation of NO[J]. Chemical Engineering Science, 2024, 285: 119614.
- [14] Xia Q, Liu X, Li H, et al. Construction of the Z-scheme Cu₂O-Ag/AgBr heterostructures to enhance the visible-light-driven photocatalytic water disinfection and antibacterial performance[J]. Journal of Alloys and Compounds, 2024, 980: 173665.
- [15] Dang J, Guo J, Wang L, et al. Construction of Z-scheme Fe₃O₄/BiOCl/BiOI heterojunction with superior recyclability for improved photocatalytic activity towards tetracycline degradation[J]. Journal of Alloys and Compounds, 2022, 893: 162251.
- [16] Beirami P, Derakhshanfard F, Gharbani P, et al. Visible-light photocatalytic removal of betamethasone using heterogeneous $CdSe/Bi_2MoO_6/g-C_3N_5$ nanophotocatalyst: Synthesis, characterization, Thermodynamic and kinetics analysis[J]. Journal of Photochemistry and Photobiology A: Chemistry, 2023, 444: 114910.
- [17] Liu J, Jiang L, Zhang H, et al. Construction of high-proportion dual bismuth-based Z-scheme

- Bi₃O₄Cl/Bi₂MoO₆ photocatalytic system via in-situ growth of Bi₂MoO₆ on Bi₃O₄Cl for enhanced photocatalytic degradation of organic pollutants[J]. Journal of Alloys and Compounds, 2023, 956: 170375.
- [18] Zhong S, Wang Y, Chen Y, et al. Improved piezo-photocatalysis for aquatic multi-pollutant removal via BiOBr/BaTiO₃ heterojunction construction[J]. Chemical Engineering Journal, 2024, 488: 151002.
- [19] Zhang Y, Zhai X, Wang N, et al. Visible light driven BiOBr/ZIF-67 S-scheme heterojunction as a novel effective marine biofouling inhibitor[J]. Journal of Environmental Chemical Engineering, 2024, 12(2): 112163.
- [20] Chen J, Xiao X, Wang Y, et al. AgI nanoparticles decorated Bi_3O_4Cl microspheres: An efficient Z-scheme heterojunction photocatalyst for the degradation of rhodamine B and tetracycline[J]. Solid State Sciences, 2020, 107: 106357.
- [21] Tang M, Ao Y, Wang P, et al. All-solid-state Z-scheme WO₃ nanorod/ZnIn₂S₄ composite photocatalysts for the effective degradation of nitenpyram under visible light irradiation[J]. Journal of Hazardous Materials, 2020, 387: 121713.
- [22] Zhang Y, Chen D, Li N, et al. Fabricating 1D/2D Co₃O₄/ZnIn₂S₄ core—shell heterostructures with boosted charge transfer for photocatalytic hydrogen production[J]. Applied Surface Science, 2023, 610: 155272
- [23] Pang B, Miao J, Wang H, et al. Construction of fast charge-transferred 0D/2D BiOBr/Bi₂WO₆ S-scheme heterojunction with enhanced photocatalytic performance[J]. Applied Surface Science, 2024, 649: 159104.
- [24] Sun X, Zhai H, Sun Z, et al. From one to three: in-situ transformation of Bi_3O_4Cl to Bi/Bi_3O_4Cl core-shell nanocomposites with highly photocatalytic activities[J]. Surfaces and Interfaces, 2023, 40: 103017.
- [25] Moghimian S, Azarmi F, Sangpour P, et al. Enhanced photocatalytic reduction of Cr(VI) using Ag@AgCl/RGO/CuO nanocomposite under visible light[J]. Journal of Photochemistry and Photobiology A: Chemistry, 2024, 452: 115584.
- [26] Song Y, Liu J, Wang X, et al. One-dimensional Bi_2MoO_6 nanosheets/ TiO_2 hollow tubes: Controllable synthesis and enhanced visible photocatalytic activity[J]. Optical Materials, 2024, 148: 114825.